Formation of PBHs: Possibilities and consequences

L. Sriramkumar

Centre for Strings, Gravitation and Cosmology, Department of Physics,
Indian Institute of Technology Madras, Chennai

Neutron Stars: The Celestial Clocks that Probe Extreme Physics

The Institute of Mathematical Sciences, Chennai

February 1–3, 2023

Plan of the talk

This talk is based on. . .

- M. Braglia, D. K. Hazra, F. Finelli, G. F. Smoot, L. Sriramkumar and A. A. Starobinsky, *Generating PBHs and small-scale GWs in two-field models of inflation*, JCAP **08**, 001 (2020) [arXiv:2005.02895 [astro-ph.CO]].
- H. V. Ragavendra, P. Saha, L. Sriramkumar and J. Silk, *PBHs and secondary GWs from ultra slow roll and punctuated inflation*, Phys. Rev. D **103**, 083510 (2021) [arXiv:2008.12202 [astro-ph.CO]].
- H. V. Ragavendra, L. Sriramkumar and J. Silk, *Could PBHs and secondary GWs have originated from squeezed initial states?*, JCAP **05**, 010 (2021) [arXiv:2011.09938 [astro-ph.CO]].
- H. V. Ragavendra and L. Sriramkumar, *Observational imprints of enhanced scalar power on small scales in ultra slow roll inflation and associated non-Gaussianities*, arXiv:2301.08887 [astro-ph.CO], invited review for Galaxies.

Plan of the talk

The horizon problem

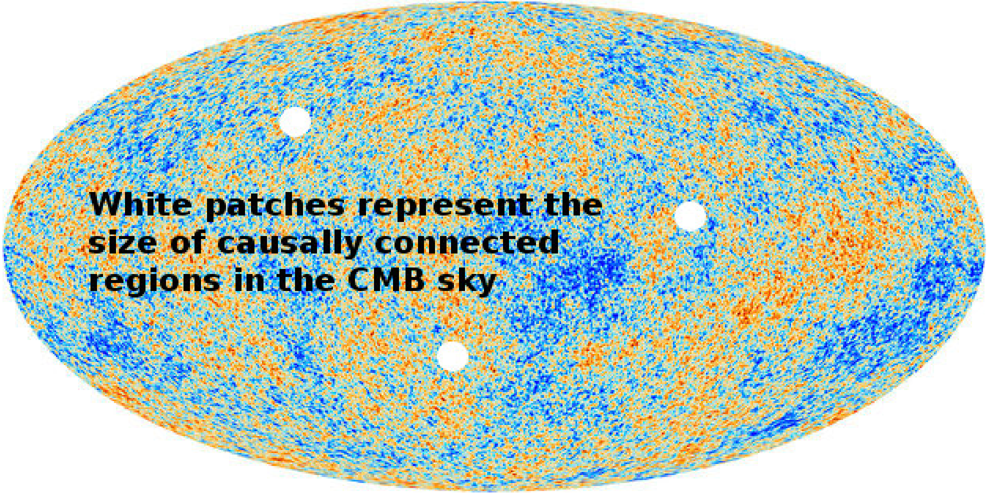

The radiation from the CMB arriving at us from regions separated by more than the Hubble radius at the last scattering surface, which subtends an angle of about 1° today, could not have interacted before decoupling.

The resolution of the horizon problem in the inflationary scenario

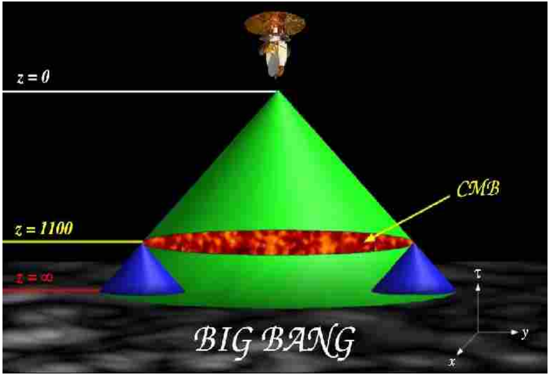

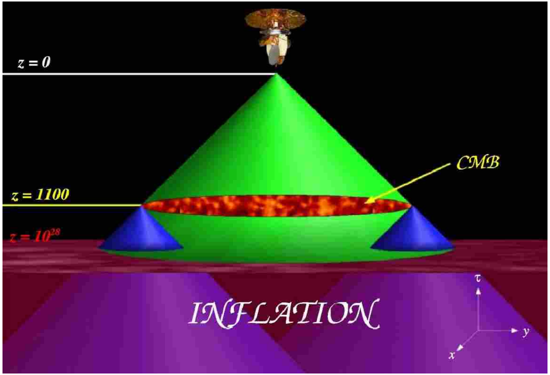

Another illustration of the horizon problem (on the left), and an illustration of its resolution (on the right) through an early and sufficiently long epoch of inflation[1].

[1] Images from W. Kinney, astro-ph/0301448.

Bringing the modes inside the Hubble radius

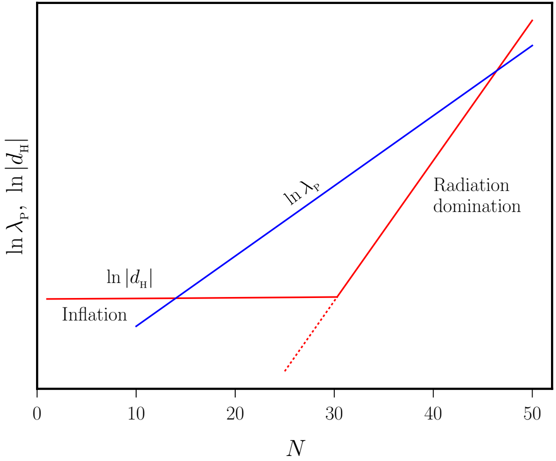

Evolution of comoving lengths

The physical wavelength $\lambda_{\rm P} \propto a$ (in blue) and the Hubble radius $d_{\rm H} = H^{-1}$ (in red) in the inflationary scenario[2]. The scale factor is expressed in terms of e-folds N as $a(N) \propto {\rm e}^{N}$.

[2] See, for example, E. W. Kolb and M. S. Turner, *The Early Universe* (Addison-Wesley Publishing Company, New York, 1990), Fig. 8.4.

Driving inflation with scalar fields

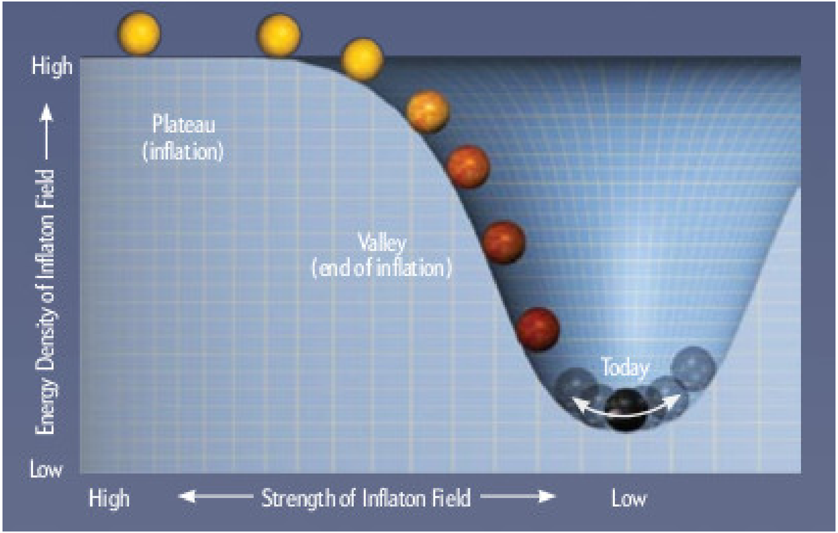

Inflation can be achieved with scalar fields encountered in high energy physics[3].

[3]Image from P. J. Steinhardt, Sci. Am. **304**, 34 (2011).

A variety of potentials to choose from

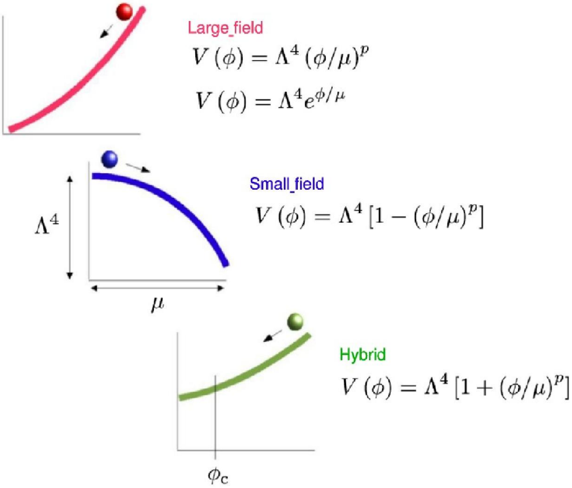

A variety of scalar field potentials have been considered to drive inflation[4]. Often, these potentials are classified as small field, large field and hybrid models.

[4] Image from W. Kinney, astro-ph/0301448.

Proliferation of inflationary models

5-dimensional assisted inflation
anisotropic brane inflation
anomaly-induced inflation
assisted inflation
assisted chaotic inflation
boundary inflation
brane inflation
brane-assisted inflation
brane gas inflation
brane-antibrane inflation
braneworld inflation
Brans-Dicke chaotic inflation
Brans-Dicke inflation
bulky brane inflation
chaotic hybrid inflation
chaotic inflation
chaotic new inflation
D-brane inflation
D-term inflation
dilaton-driven inflation
dilaton-driven brane inflation
double inflation
double D-term inflation
dual inflation
dynamical inflation
dynamical SUSY inflation
eternal inflation
extended inflation
extended open inflation
extended warm inflation
extra dimensional inflation
F-term inflation
F-term hybrid inflation
false vacuum inflation
false vacuum chaotic inflation
fast-roll inflation
first order inflation
gauged inflation
generalised inflation
generalized assisted inflation
generalized slow-roll inflation
gravity driven inflation
Hagedorn inflation
higher-curvature inflation
hybrid inflation
hyperextended inflation
induced gravity inflation
induced gravity open inflation
intermediate inflation
inverted hybrid inflation
isocurvature inflation
K inflation
kinetic inflation
lambda inflation
large field inflation
late D-term inflation
late-time mild inflation
low-scale inflation
low-scale supergravity inflation
M-theory inflation
mass inflation
massive chaotic inflation
moduli inflation
multi-scalar inflation
multiple inflation
multiple-field slow-roll inflation
multiple-stage inflation
natural inflation
natural Chaotic inflation
natural double inflation
natural supergravity inflation
new inflation
next-to-minimal supersymmetric hybrid inflation
non-commutative inflation
non-slow-roll inflation
nonminimal chaotic inflation
old inflation
open hybrid inflation
open inflation
oscillating inflation
polynomial chaotic inflation
polynomial hybrid inflation
power-law inflation
pre-Big-Bang inflation
primary inflation
primordial inflation
quasi-open inflation
quintessential inflation
R-invariant topological inflation
rapid asymmetric inflation
running inflation
scalar-tensor gravity inflation
scalar-tensor stochastic inflation
Seiberg-Witten inflation
single-bubble open inflation
spinodal inflation
stable starobinsky-type inflation
steady-state eternal inflation
steep inflation
stochastic inflation
string-forming open inflation
successful D-term inflation
supergravity inflation
supernatural inflation
superstring inflation
supersymmetric hybrid inflation
supersymmetric inflation
supersymmetric topological inflation
supersymmetric new inflation
synergistic warm inflation
TeV-scale hybrid inflation

A (partial?) list of ever-increasing number of inflationary models[5]. Actually, it may not even be possible to rule out some of these models!

[5] From E. P. S. Shellard, *The future of cosmology: Observational and computational prospects*, in *The Future of Theoretical Physics and Cosmology*, Eds. G. W. Gibbons, E. P. S. Shellard and S. J. Rankin (Cambridge University Press, Cambridge, England, 2003).

From inside the Hubble radius to super-Hubble scales

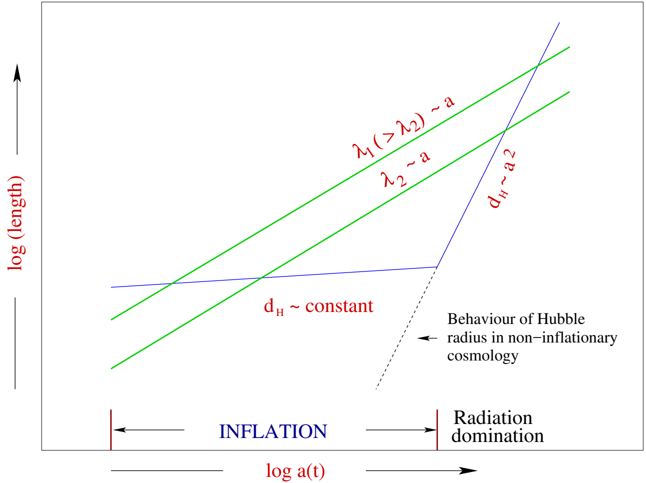

Back to formation of PBHs

The initial conditions are imposed in the sub-Hubble regime when the modes are well inside the Hubble radius (*viz.* when $k/(a\,H) \gg 1$) and the power spectra are evaluated when they sufficiently outside (*i.e.* as $k/(a\,H) \ll 1$).

Typical evolution of the perturbations

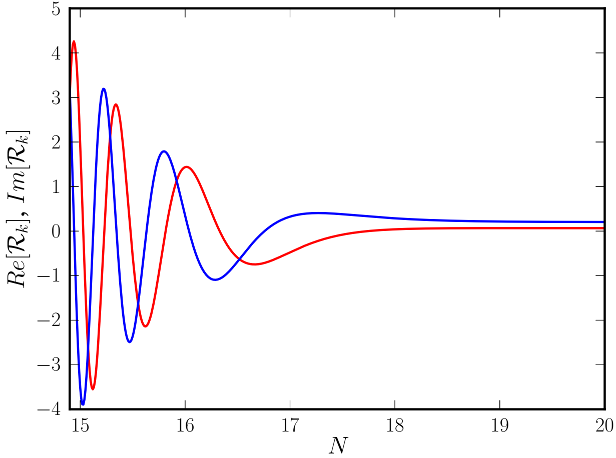

Typical evolution of the real and the imaginary parts of the scalar modes during slow roll inflation. The mode considered here leaves the Hubble radius at about 18 e-folds[6].

[6]Figure from V. Sreenath, *Computation and characteristics of inflationary three-point functions*, Ph.D. Thesis, Indian Institute of Technology Madras, Chennai, India (2015).

Spectral indices and the tensor-to-scalar ratio

The scalar and tensor power spectra, viz. $\mathcal{P}_{_{\rm S}}(k)$ and $\mathcal{P}_{_{\rm T}}(k)$, can be expressed in terms of the Fourier modes f_k and g_k as follows:

$$\mathcal{P}_{_{\rm S}}(k) = \frac{k^3}{2\,\pi^2}\,|f_k(\eta_{\rm e})|^2,$$

$$\mathcal{P}_{_{\rm T}}(k) = 8\,\frac{k^3}{2\,\pi^2}\,|g_k(\eta_{\rm e})|^2,$$

with $\eta_{\rm e}$ corresponding to suitably late times during inflation.

While comparing with the observations, for convenience, one often uses the following power law, template scalar and the tensor spectra:

$$\mathcal{P}_{_{\rm S}}(k) = A_{_{\rm S}}\,\left(\frac{k}{k_\ast}\right)^{n_{_{\rm S}}-1}, \qquad \mathcal{P}_{_{\rm T}}(k) = A_{_{\rm T}}\,\left(\frac{k}{k_\ast}\right)^{n_{_{\rm T}}},$$

with the spectral indices $n_{_{\rm S}}$ and $n_{_{\rm T}}$ assumed to be constant. The tensor-to-scalar ratio r is defined as

$$r(k) = \frac{\mathcal{P}_{_{\rm T}}(k)}{\mathcal{P}_{_{\rm S}}(k)}.$$

Plan of the talk

CMB angular power spectrum from Planck

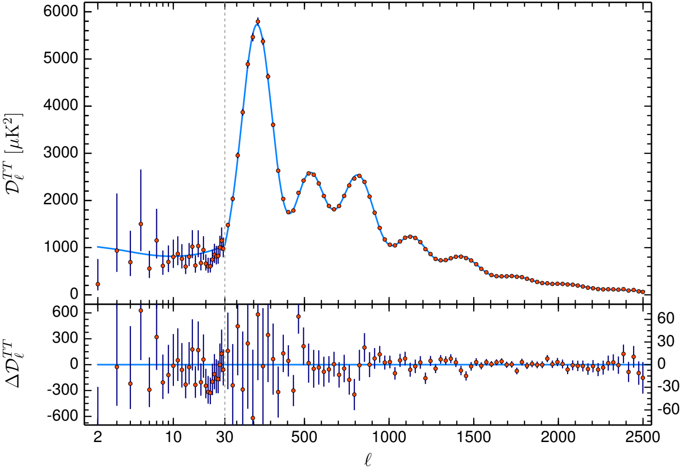

The CMB TT angular power spectrum from the Planck 2018 data (red dots with error bars) and the best fit ΛCDM model with a power law primordial spectrum (solid blue curve)[7].

[7] Planck Collaboration (N. Aghanim *et al.*), Astron. Astrophys. **641**, A6 (2020).

Performance of inflationary models in the $n_{\rm s}$-r plane

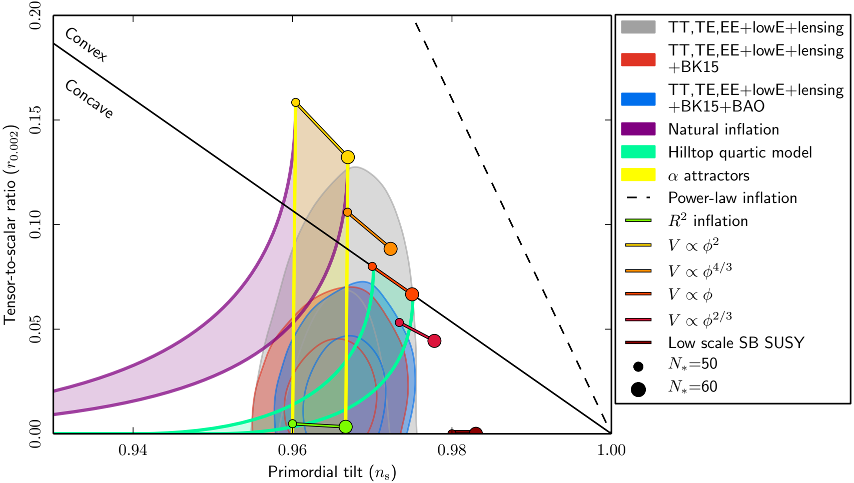

Joint constraints on $n_{\rm s}$ and $r_{0.002}$ from Planck in combination with other data sets, compared to the theoretical predictions of some of the popular inflationary models[8].

[8] Planck Collaboration (Y. Akrami *et al.*), Astron. Astrophys. **641**, A10 (2020).

Spectra leading to an improved fit to the CMB data

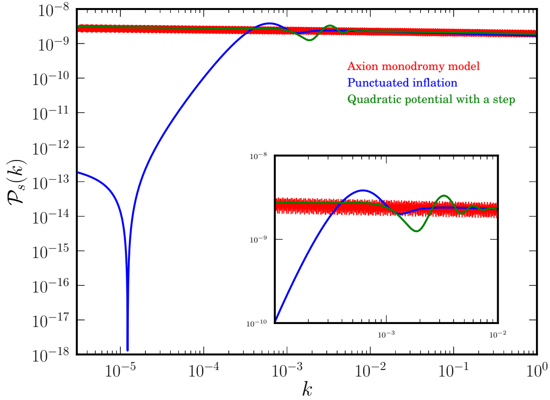

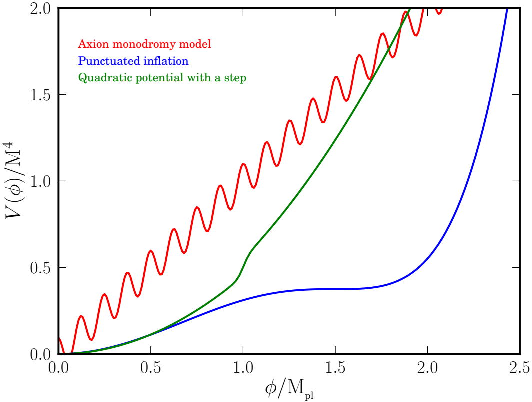

The scalar power spectra (on the left) arising in different inflationary models (on the right) that lead to a better fit to the CMB data than the conventional power law spectrum[9].

[9] R. K. Jain, P. Chingangbam, J.-O. Gong, L. Sriramkumar and T. Souradeep, JCAP **01**, 009 (2009);
D. K. Hazra, M. Aich, R. K. Jain, L. Sriramkumar and T. Souradeep, JCAP **10**, 008 (2010);
M. Aich, D. K. Hazra, L. Sriramkumar and T. Souradeep, Phys. Rev. D **87**, 083526 (2013).

Plan of the talk

Behavior of the comoving wave number and Hubble radius

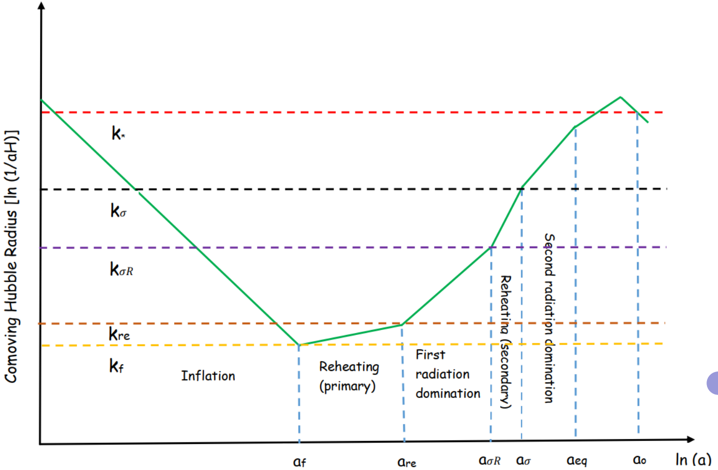

Evolution of physical lengths

Behavior of the comoving wave number k (horizontal lines in different colors) and the comoving Hubble radius $d_{\rm H}/a = (a\,H)^{-1}$ (in green) across different epochs[10].

[10] Md. R. Haque, D. Maity, T. Paul and L. Sriramkumar, Phys. Rev. D **104**, 063513 (2021).

Formation of BHs in the early universe

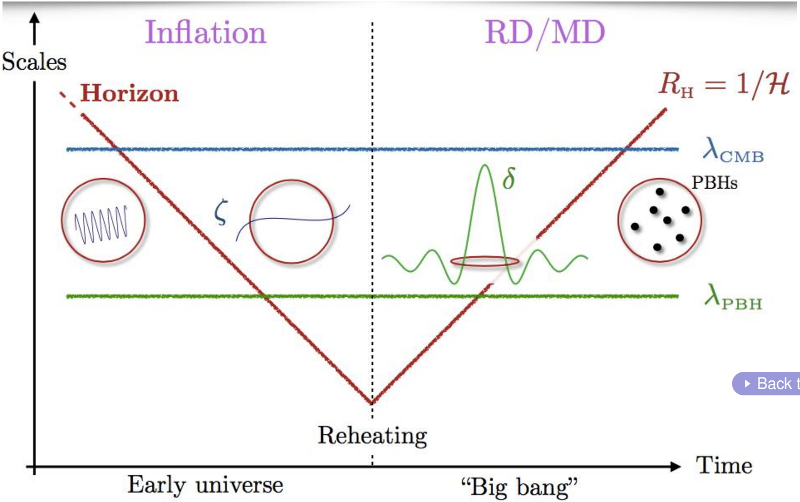

Back to calculation of $f_{\rm PBH}$

BHs can form when perturbations with significant amplitudes reenter the Hubble radius during the radiation dominated epoch[11].

[11] Figure from G. Franciolini, arXiv:2110.06815 [astro-ph.CO].

Amplitude required to form significant number of PBHs

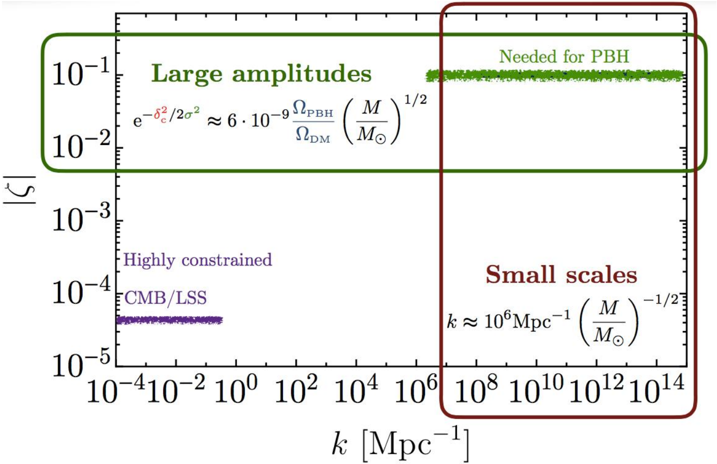

In order to form significant number of black holes, the amplitude of the perturbations on small scales has to be large enough such that the dimensionless amplitude of the scalar perturbation is close to unity[12].

[12] Figure credit G. Franciolini.

Potentials admitting ultra slow roll inflation

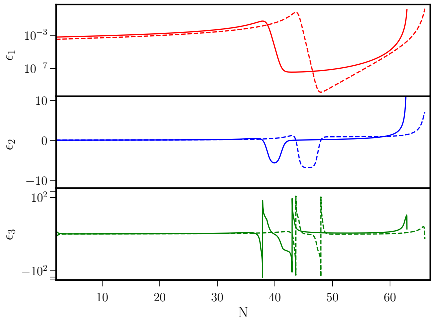

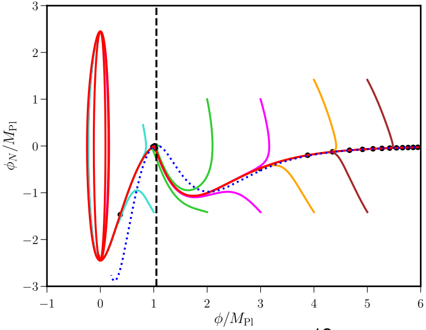

Potentials leading to ultra slow roll inflation (with $x = \phi/v$, v being a constant)[13]:

$$\mathrm{USR1}: V(\phi) = V_0\, \frac{6\,x^2 - 4\,\alpha\,x^3 + 3\,x^4}{(1+\beta\,x^2)^2},$$

$$\mathrm{USR2}: V(\phi) = V_0\, \left\{\tanh\left(\frac{\phi}{\sqrt{6}\,M_{_{\rm Pl}}}\right) + A\,\sin\left[\frac{\tanh\left[\phi/\left(\sqrt{6}\,M_{_{\rm Pl}}\right)\right]}{f_\phi}\right]\right\}^2.$$

[13] J. Garcia-Bellido and E. R. Morales, Phys. Dark Univ. **18**, 47 (2017);
I. Dalianis, A. Kehagias and G. Tringas, JCAP **01**, 037 (2019).

Potentials permitting punctuated inflation

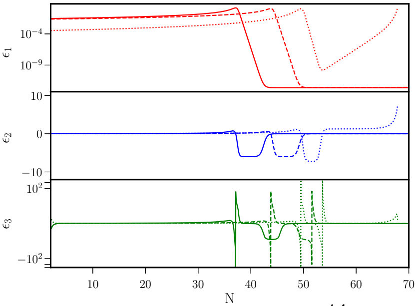

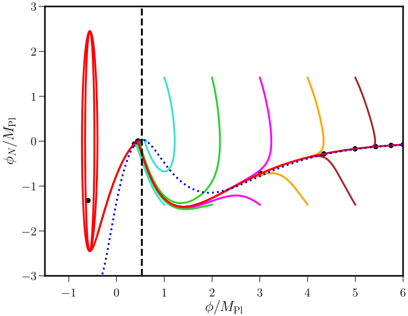

Potentials admitting punctuated inflation[14]:

$$\mathrm{PI1}: V(\phi) = V_0\,\left(1 + B\,\phi^4\right), \quad \mathrm{PI2}: V(\phi) = \frac{m^2}{2}\,\phi^2 - \frac{2\,m^2}{3\,\phi_0}\,\phi^3 + \frac{m^2}{4\,\phi_0^2}\,\phi^4,$$

$$\mathrm{PI3}: V(\phi) = V_0\,\left[c_0 + c_1\,\tanh\left(\frac{\phi}{\sqrt{6\,\alpha}\,M_{\rm Pl}}\right) + c_2\,\tanh^2\left(\frac{\phi}{\sqrt{6\,\alpha}\,M_{\rm Pl}}\right) + c_3\,\tanh^3\left(\frac{\phi}{\sqrt{6\,\alpha}\,M_{\rm Pl}}\right)\right]^2.$$

[14] D. Roberts, A. R. Liddle and D. H. Lyth, Phys. Rev. D **51**, 4122 (1995);
R. K. Jain, P. Chingangbam, J.-O. Gong, L. Sriramkumar and T. Souradeep, JCAP **01**, 009 (2009);
I. Dalianis, A. Kehagias and G. Tringas, JCAP **01**, 037 (2019).

Reconstructing scenarios of ultra slow roll and punctuated inflation

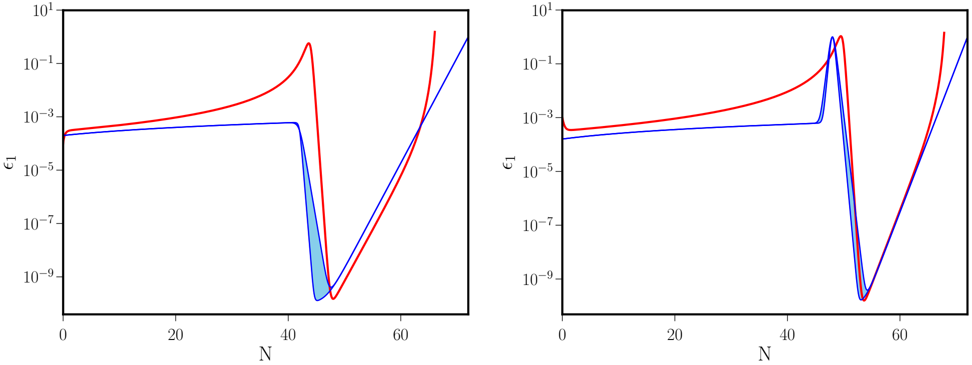

Behavior of the first slow roll parameter $\epsilon_1(N)$ leading to ultra slow and punctuated inflation[15]:

$$\text{RSI}: \epsilon_1^{\text{I}}(N) = [\epsilon_{1a}\ (1+\epsilon_{2a}\, N)] \left[1-\tanh\left(\frac{N-N_1}{\Delta N_1}\right)\right] + \epsilon_{1b} + \exp\left(\frac{N-N_2}{\Delta N_2}\right),$$

$$\text{RSII}: \epsilon_1^{\text{II}}(N) = \epsilon_1^{\text{I}}(N) + \cosh^{-2}\left(\frac{N-N_1}{\Delta N_1}\right).$$

Back to $f_{\rm PBH}$

[15] H. V. Ragavendra, P. Saha, L. Sriramkumar and J. Silk, Phys. Rev. D **103**, 083510 (2021).

Power spectra in the inflationary models and reconstructed scenarios

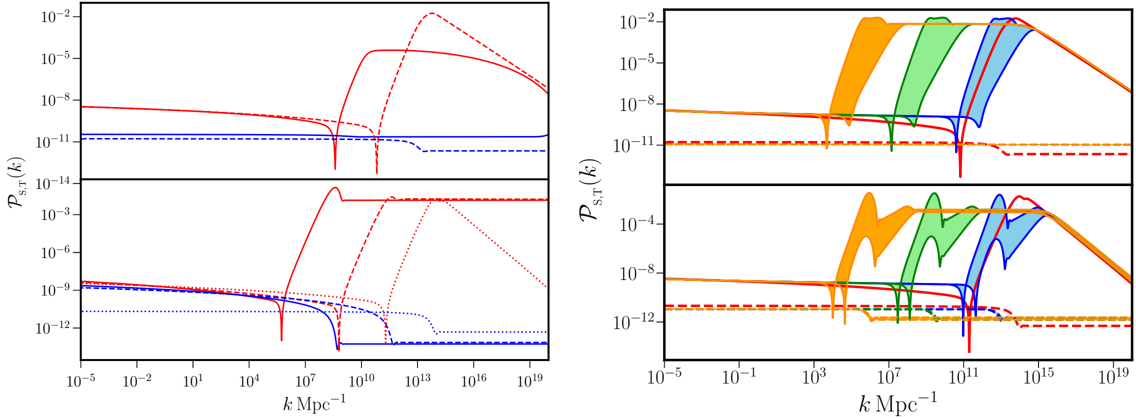

The scalar and the tensor power spectra arising in the various inflationary models (in red and blue on the left) and the reconstructed scenarios (in blue, green and orange, on the right)[16].

[16] H. V. Ragavendra, P. Saha, L. Sriramkumar and J. Silk, Phys. Rev. D **103**, 083510 (2021).

The two field model of interest

It has been noticed that two scalar fields ϕ and χ governed by the following action:

$$S[\phi, \chi] = \int \mathrm{d}^4x \sqrt{-g} \left[-\frac{1}{2}\, \partial^\mu\phi\, \partial_\mu\phi - \frac{f(\phi)}{2}\, \partial^\mu\chi\, \partial_\mu\chi - V(\phi, \chi)\right]$$

described by a potential such as

$$V(\phi,\, \chi) = V_0\, \frac{\phi^2}{\phi_0^2 + \phi^2} + \frac{m_\chi^2}{2}\, \chi^2$$

and the non-canonical coupling functions

$$f_1(\phi) = \mathrm{e}^{2\, b_1\, \phi} \quad \text{or} \quad f_2(\phi) = \mathrm{e}^{2\, b_2\, \phi^2}$$

can lead to features in the scalar power spectrum[17].

[17] M. Braglia, D. K. Hazra, L. Sriramkumar and F. Finelli, JCAP **08** 025 (2020).

Behavior of the scalar fields and the first slow roll parameter

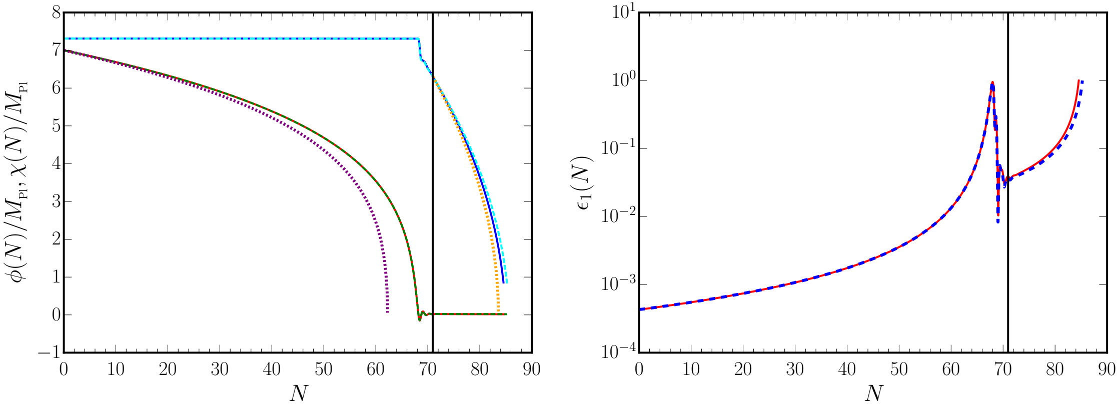

Behavior of the two scalar fields ϕ and χ (in blue and red, on the left) and the first slow roll parameter ϵ_1 (on the right) in the two field model of our interest[18]. Note that there arises a turn in the field space around $N = 70$, when the first slow roll parameter begins to decrease before increasing again, leading to the termination of inflation.

[18] M. Braglia, D. K. Hazra, F. Finelli, G. F. Smoot, L. Sriramkumar and A. A. Starobinsky, JCAP **08**, 001 (2020).

Enhanced power on small scales in two field models

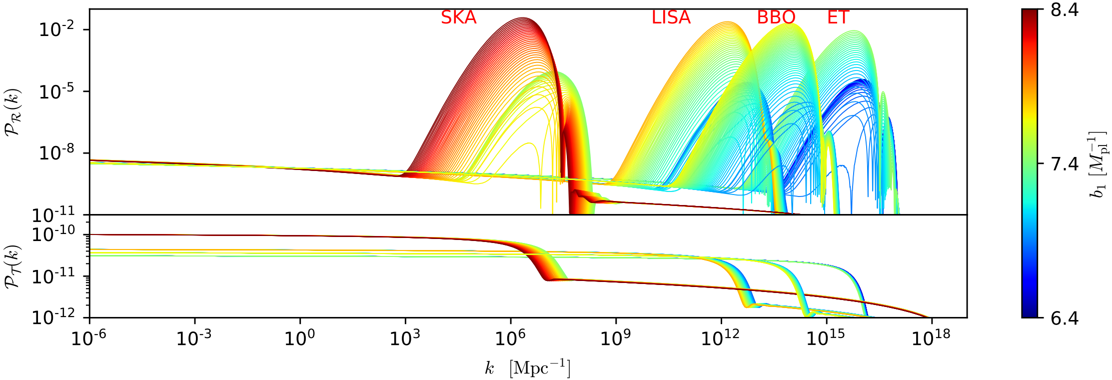

The scalar (on top) and the tensor (at the bottom) power spectra evaluated at the end of inflation have been plotted for a few different sets of initial conditions for the fields and a range of values of the parameter b_1[19].

[19] M. Braglia, D. K. Hazra, F. Finelli, G. F. Smoot, L. Sriramkumar and A. A. Starobinsky, JCAP **08**, 001 (2020).

Plan of the talk

Calculation of $f_{\rm PBH}(M)$ I

During the radiation dominated epoch, the matter power spectrum $\mathcal{P}_\delta(k)$ and the inflationary scalar power spectrum $\mathcal{P}_{\rm S}(k)$ are related through the expression

$$\mathcal{P}_\delta(k) = \frac{16}{81}\left(\frac{k}{a\,H}\right)^4 \mathcal{P}_{\rm S}(k).$$

▸ Formation of PBHs

Let the variance σ^2 in the spatial density fluctuations be smoothed over the scale R with the aid of a window function $W(k\,R)$. In such a case, the variance $\sigma^2(R)$ can be written as[20]

$$\sigma^2(R) = \int_0^\infty \frac{{\rm d}k}{k}\,\mathcal{P}_\delta(k)\,W^2(k\,R).$$

We shall work with a Gaussian window function of the form $W(k\,R) = {\rm e}^{-(k^2\,R^2)/2}$.

[20] See,for example, B. Carr, F. Kuhnel and M. Sandstad, Phys. Rev. D **94**, 083504 (2016); B. Carr and F. Kuhnel, Ann. Rev. Nucl. Part. Sci. **70**, 355 (2020).

Calculation of $f_{\rm PBH}(M)$ II

If $M_{\rm H}$ denotes the mass within the Hubble radius H^{-1}, it is reasonable to suppose that a certain fraction of the total mass within the Hubble radius, say, $M = \gamma_*\, M_{\rm H}$, goes on to form PBHs when a mode with wave number k reenters the Hubble radius.

It seems natural to choose $k = R^{-1}$ and, in such a case, one can show that R and M are related as follows:

$$R = 4.72 \times 10^{-7}\, \left(\frac{\gamma_*}{0.2}\right)^{-1/2}\, \left(\frac{g_{*,k}}{g_{*,{\rm eq}}}\right)^{1/12}\, \left(\frac{M}{M_\odot}\right)^{1/2}\, {\rm Mpc}.$$

One assumes that the density contrast in matter characterized by the quantity δ is a Gaussian random variable described by the probability density

$$P(\delta) = \frac{1}{\sqrt{2\,\pi\,\sigma^2}}\, \exp\left(-\frac{\delta^2}{2\,\sigma^2}\right),$$

where σ^2 is the variance of the spatial density fluctuations.

Calculation of $f_{\rm PBH}(M)$ III

Let us further assume that perturbations with a density contrast beyond a certain threshold, say, $\delta_{\rm c}$, are responsible for the formation of PBHs. In such a case, the fraction, say, β, of the density fluctuations that collapse to form PBHs is described by the integral

$$\beta(M) = \int_{\delta_{\rm c}}^{1} {\rm d}\delta\, P(\delta) \simeq \frac{1}{2}\left[1 - {\rm erf}\left(\frac{\delta_{\rm c}}{\sqrt{2\,\sigma^2(M)}}\right)\right],$$

where ${\rm erf}(z)$ denotes the error function[21]. On using the above arguments, we can obtain the fraction of PBHs, say, $f_{\rm PBH}$, contributing to the dark matter density today, to be

$$f_{\rm PBH}(M) = 2^{1/4}\,\gamma_\ast^{3/2}\,\beta(M)\,\left(\frac{\Omega_{\rm m}\,h^2}{\Omega_{\rm c}\,h^2}\right)\left(\frac{g_{\ast,k}}{g_{\ast,{\rm eq}}}\right)^{-1/4}\left(\frac{M}{M_{\rm eq}}\right)^{-1/2},$$

where $\Omega_{\rm m}$ and $\Omega_{\rm c}$ are the dimensionless parameters describing the matter and cold matter densities, with the Hubble parameter, as usual, expressed as $H_0 = 100\,h\,{\rm km\,sec}^{-1}\,{\rm Mpc}^{-1}$.

[21] See, for instance, B. Carr and J. Silk, Mon. Not. Roy. Astron. Soc. **478**, 3756 (2018); M. Sasaki, T. Suyama, T. Tanaka and S. Yokoyama, Class. Quant. Grav. **35**, 063001 (2018).

Time scale of evaporation of PBHs

Recall that BHs of mass M emit Hawking radiation which is thermal in nature, with the temperature

$$k_{\rm B}\, T = \frac{\hbar\, c^3}{4\,\pi\, M}.$$

These black holes will evaporate over a time scale of

$$t_{\rm ev} = \frac{60\, G^2\, M^3}{\pi^3\, \hbar\, c^4}\, \left(\frac{M}{M_\odot}\right)^3 = 2.5 \times 10^{63}\, \left(\frac{M}{M_\odot}\right)^3\ {\rm yrs.}$$

This implies that PBHs with mass $M \lesssim 10^{-18}\, M_\odot$ would have evaporated by now.

Constraints on $f_{\rm PBH}(M)$

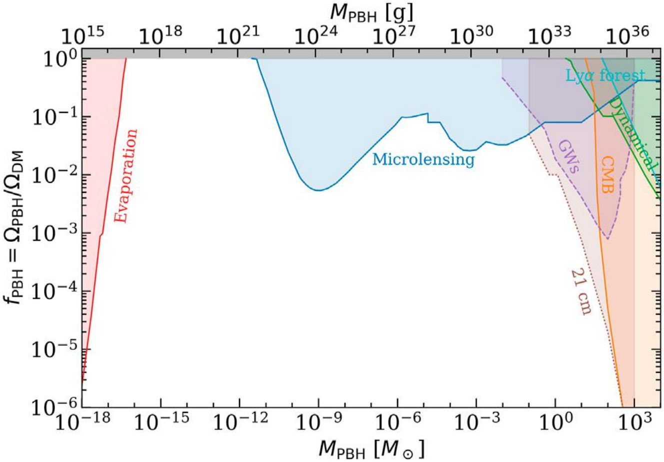

Observational constraints on the quantity $f_{\rm PBH}$, i.e. the fractional energy density of PBHs that constitute cold dark matter today[22].

[22] P. Villanueva-Domingo, O. Mena and S. Palomares-Ruiz, Front. Astron. Space Sci. **8**, 681084 (2021);
For latest constraints, see https://github.com/bradkav/PBHbounds/blob/master/README.md.

$f_{\rm PBH}(M)$ in ultra slow roll and punctuated inflation

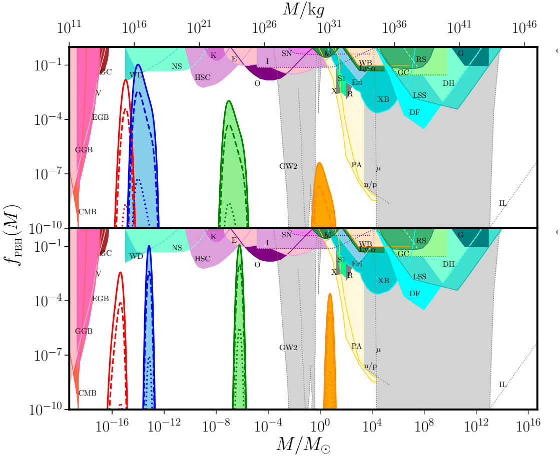

The fraction of PBHs contributing to the dark matter density today $f_{\rm PBH}(M)$ has been plotted for the various models and scenarios of interest, viz. USR2 and RS1 (on top, in red and blue) and PI3 and RS2 (at the bottom, in red and blue)[23].

[23] H. V. Ragavendra, P. Saha, L. Sriramkumar and J. Silk, Phys. Rev. D **103**, 083510 (2021).

Illustrating the $f_{\rm PBH}(M) \propto M^{-1/2}$ behavior

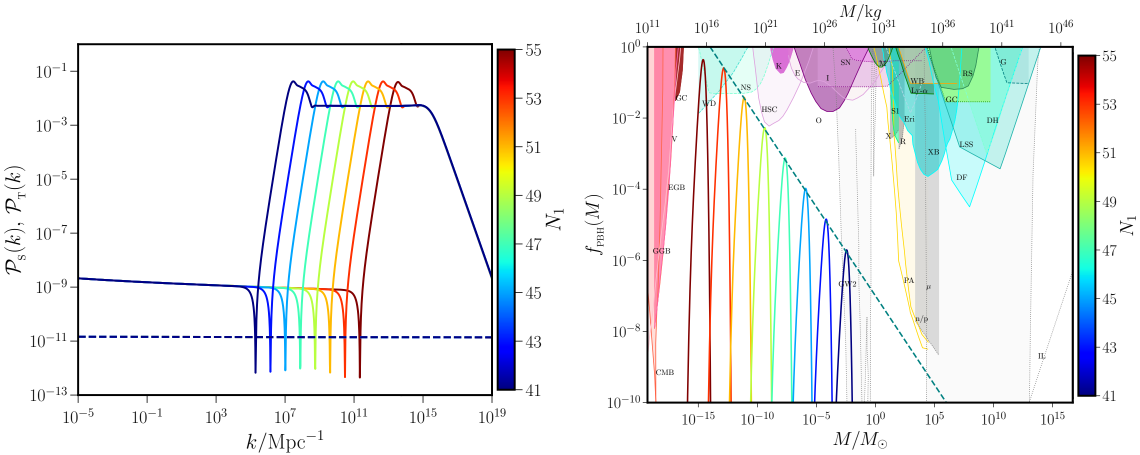

The quantity $f_{\rm PBH}(M)$ (on the right) corresponding to scalar spectra generated in the reconstructed scenarios (on the left) have been illustrated. We find that $f_{\rm PBH}(M)$ behaves as $M^{-1/2}$ (in dashed teal, on the right), as expected[24].

▸ Reconstructed scenarios

[24] H. V. Ragavendra and L. Sriramkumar, arXiv:2301.08887 [astro-ph.CO], invited review for Galaxies.

$f_{\rm PBH}(M)$ in the two field model

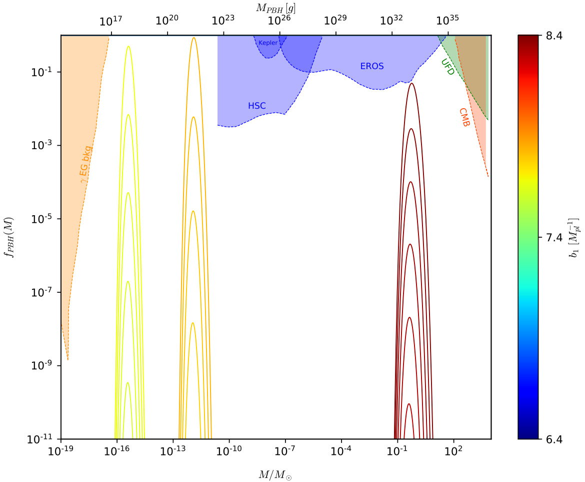

The fraction of PBHs contributing to the dark matter density today $f_{\rm PBH}(M)$ in the two field model of our interest[25].

[25] M. Braglia, D. K. Hazra, F. Finelli, G. F. Smoot, L. Sriramkumar and A. A. Starobinsky, JCAP **08**, 001 (2020).

GWs sourced by second order scalar perturbations I

At the second order in the perturbations, one finds that the equation governing the tensor modes, say, $h_{\boldsymbol{k}}$, can be written as[26]

$$h_{\boldsymbol{k}}^{\lambda\,\prime\prime} + 2\,\mathcal{H}\,h_{\boldsymbol{k}}^{\lambda\,\prime} + k^2\,h_{\boldsymbol{k}}^{\lambda} = S_{\boldsymbol{k}}^{\lambda}$$

with the source term $S_{\boldsymbol{k}}^{\lambda}$ being given by

$$S_{\boldsymbol{k}}^{\lambda}(\eta) = 4\int\frac{\mathrm{d}^3\boldsymbol{p}}{(2\,\pi)^{3/2}}\,e^{\lambda}(\boldsymbol{k},\boldsymbol{p})\,\biggl\{2\,\Psi_{\boldsymbol{p}}(\eta)\,\Psi_{\boldsymbol{k}-\boldsymbol{p}}(\eta) + \frac{4}{3\,(1+w)\,\mathcal{H}^2}\,\left[\Psi_{\boldsymbol{p}}'(\eta)+\mathcal{H}\,\Psi_{\boldsymbol{p}}(\eta)\right]\,\left[\Psi_{\boldsymbol{k}-\boldsymbol{p}}'(\eta)+\mathcal{H}\,\Psi_{\boldsymbol{k}-\boldsymbol{p}}(\eta)\right]\biggr\},$$

where $\Psi_{\boldsymbol{k}}$ represents the Fourier modes of the Bardeen potential, while $\mathcal{H}$ and w denote the conformal Hubble parameter and the equation of state parameter describing the universe at the conformal time η. Also, $e^{\lambda}(\boldsymbol{k},\boldsymbol{p}) = e_{ij}^{\lambda}(\boldsymbol{k})\,p^i\,p^j$, with $e_{ij}^{\lambda}(\boldsymbol{k})$ representing the polarization of the tensor perturbations.

[26] K. N. Ananda, C. Clarkson and D. Wands, Phys. Rev. D **75**, 123518 (2007);
D. Baumann, P. J. Steinhardt, K. Takahashi and K. Ichiki, Phys. Rev. D **76**, 084019 (2007).

GWs sourced by second order scalar perturbations II

During radiation domination, we can express the Fourier modes $\Psi_{\boldsymbol{k}}$ of the Bardeen potential in terms of the inflationary Fourier modes $\mathcal{R}_{\boldsymbol{k}}$ of the curvature perturbations generated during inflation through the relation

$$\Psi_{\boldsymbol{k}}(\eta) = \frac{2}{3}\,\mathcal{T}(k\,\eta)\,\mathcal{R}_{\boldsymbol{k}},$$

where $\mathcal{T}(k\,\eta)$ is the transfer function given by

$$\mathcal{T}(k\,\eta) = \frac{9}{(k\,\eta)^2}\left[\frac{\sin\left(k\,\eta/\sqrt{3}\right)}{k\,\eta/\sqrt{3}} - \cos\left(k\,\eta/\sqrt{3}\right)\right].$$

Spectrum of secondary GWs today

The dimensionless parameter $\Omega_{\rm GW}(k,\eta)$ describing the energy density of GWs, when evaluated at late times during the radiation dominated epoch, can be expressed as[27]

$$\Omega_{\rm GW}(k,\eta) = \frac{\rho_{\rm GW}(k,\eta)}{\rho_{\rm cr}(\eta)} = \frac{1}{972}\int_0^\infty {\rm d}v \int_{|1-v|}^{1+v} {\rm d}u \left[\frac{4\,v^2-(1+v^2-u^2)^2}{4\,u\,v}\right]^2 \mathcal{P}_{\rm S}(k\,v)\,\mathcal{P}_{\rm S}(k\,u) \times \left[\mathcal{I}_c^2(u,v)+\mathcal{I}_s^2(u,v)\right]$$

where the quantities $\mathcal{I}_c(u,v)$ and $\mathcal{I}_s(u,v)$ are determined by the transfer function $\mathcal{T}(k,\eta)$ for the scalar perturbations.

We can express $\Omega_{\rm GW}(k)$ today in terms of the above $\Omega_{\rm GW}(k,\eta)$ as follows:

$$h^2\,\Omega_{\rm GW}(k) \simeq 1.38\times 10^{-5}\left(\frac{g_{*,k}}{106.75}\right)^{-1/3}\left(\frac{\Omega_r\,h^2}{4.16\times 10^{-5}}\right)\Omega_{\rm GW}(k,\eta),$$

where $\Omega_{\rm r}$ denotes the dimensionless energy density of radiation today, while $g_{*,k}$ and $g_{*,0}$ represent the number of relativistic degrees of freedom at reentry and today, respectively.

[27] K. Kohri and T. Terada, Phys. Rev. D **97**, 123532 (2018);
J. R. Espinosa, D. Racco and A. Riotto, JCAP **09**, 012 (2018).

$\Omega_{\rm GW}(f)$ in ultra slow roll and punctuated inflation

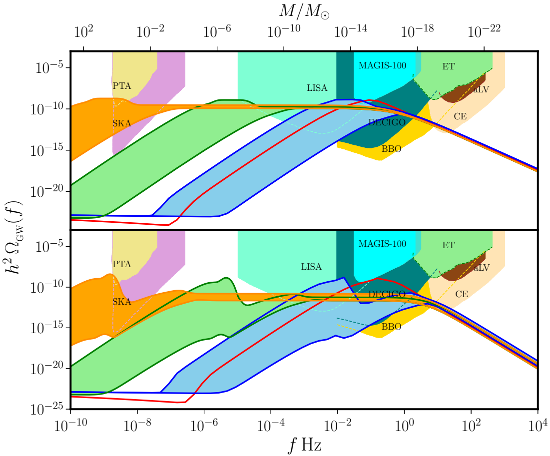

The dimensionless density parameter $\Omega_{\rm GW}$ arising in the models and reconstructed scenarios of USR2 and RS1 (in red and blue, on top) as well as PI3 and RS2 (in red and blue, at the bottom) have been plotted as a function of the frequency f[28].

[28] H. V. Ragavendra, P. Saha, L. Sriramkumar and J. Silk, Phys. Rev. D **103**, 083510 (2021).

$\Omega_{\rm GW}(f)$ in the two field model

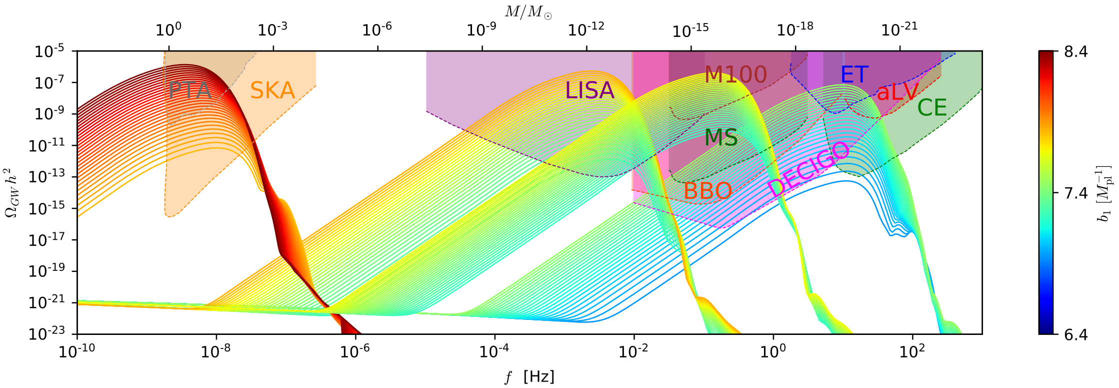

The dimensionless density parameter $\Omega_{\rm GW}(f)$ arising in the two field model has been plotted as function of frequency for a set of initial conditions for the background fields as well as a range of values of the parameter b_1[29].

[29] M. Braglia, D. K. Hazra, F. Finelli, G. F. Smoot, L. Sriramkumar and A. A. Starobinsky, JCAP **08**, 001 (2020).

Plan of the talk

Template bispectra

For comparison with the observations, the scalar bispectrum is often expressed in terms of the parameters $f_{\rm NL}^{\rm loc}$, $f_{\rm NL}^{\rm eq}$ and $f_{\rm NL}^{\rm orth}$ as follows:

$$\mathcal{B}(\boldsymbol{k}_1, \boldsymbol{k}_2, \boldsymbol{k}_3) = f_{\rm NL}^{\rm loc}\, \mathcal{B}_{\rm loc}(\boldsymbol{k}_1, \boldsymbol{k}_2, \boldsymbol{k}_3) + f_{\rm NL}^{\rm eq}\, \mathcal{B}_{\rm eq}(\boldsymbol{k}_1, \boldsymbol{k}_2, \boldsymbol{k}_3) + f_{\rm NL}^{\rm orth}\, \mathcal{B}_{\rm orth}(\boldsymbol{k}_1, \boldsymbol{k}_2, \boldsymbol{k}_3).$$

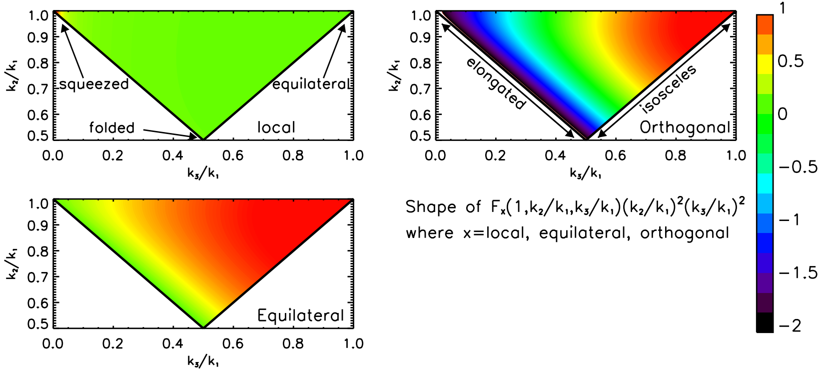

Illustration of the three template basis bispectra[30].

[30] E. Komatsu, Class. Quantum Grav. **27**, 124010 (2010).

The shape of the slow roll bispectrum

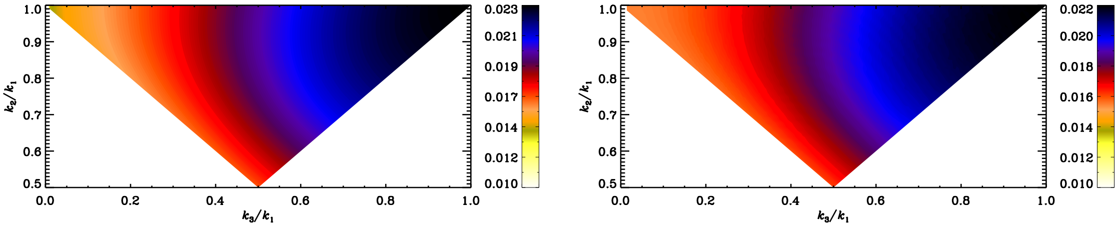

The non-Gaussianity parameter f_{NL}, evaluated in the slow roll approximation (analytically on the left and numerically on the right), has been plotted as a function of k_3/k_1 and k_2/k_1 for the case of the popular quadratic potential[31]. Note that the non-Gaussianity parameter peaks in the equilateral limit wherein $k_1 = k_2 = k_3$. In slow roll scenarios involving the canonical scalar field, the largest value of f_{NL} is found to be of the order of the first slow roll parameter ϵ_1.

[31] D. K. Hazra, L. Sriramkumar and J. Martin, JCAP **05**, 026, (2013).

Constraints on the scalar non-Gaussianity parameters

The constraints on the primordial values of the non-Gaussianity parameters from the Planck data are as follows[32]:

$$\begin{aligned} f_{\rm NL}^{\rm loc} &= -0.9 \pm 5.1, \\ f_{\rm NL}^{\rm eq} &= -26 \pm 47, \\ f_{\rm NL}^{\rm ortho} &= -38 \pm 24. \end{aligned}$$

These constraints imply that slowly rolling single field models involving the canonical scalar field which are favored by the data at the level of power spectra are also consistent with the data at the level of non-Gaussianities.

[32] Planck Collaboration (Y. Akrami *et al.*), Astron. Astrophys. **641**, A9 (2020).

The scalar bispectrum in ultra slow roll and punctuated inflation

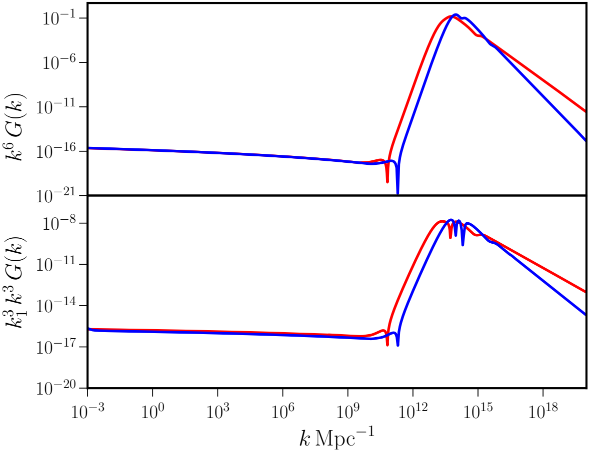

The amplitude of the dimensionless scalar bispectra has been plotted in the equilateral (on top) and squeezed limits (at the bottom) for the models USR2 (in red) and PI3 (in blue). The bispectra have approximately the same shape as the corresponding power spectra[33].

[33] H. V. Ragavendra, P. Saha, L. Sriramkumar and J. Silk, Phys. Rev. D **103**, 083510 (2021).

$f_{\rm NL}$ in ultra slow roll and punctuated inflation

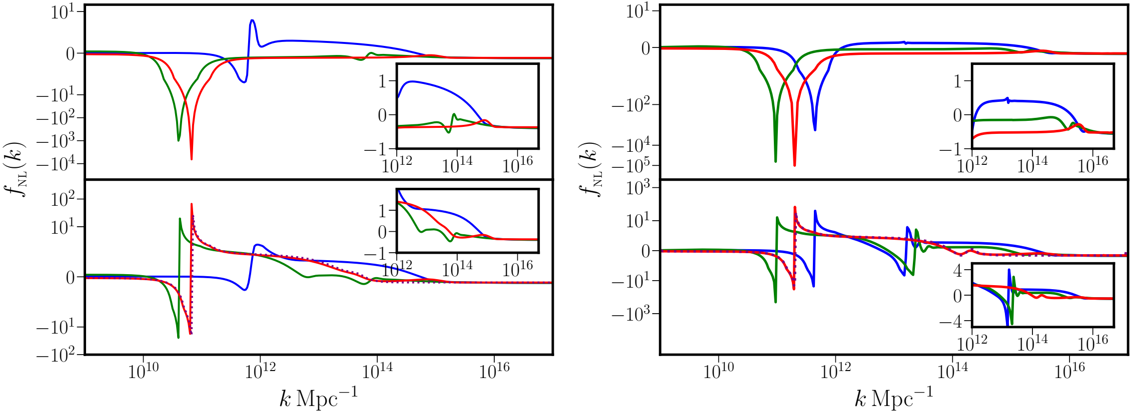

The scalar non-Gaussianity parameter $f_{\rm NL}$ has been plotted in the equilateral (on top) and the squeezed (at the bottom) limits for the models of USR2 and PI3 (in red, on the left and the right) and the reconstructed scenarios RS1 and RS2 (in blue and green, on the left and the right).

Plan of the talk

Summary

- Inflationary models permitting an epoch of ultra slow roll lead to enhanced power on small scales, resulting in significant production of PBHs and increased strengths of secondary GWs.
- The two field models require less amount of fine tuning to generate features in the primordial spectrum[34].
- The effects of non-Gaussianities on the formation of PBHs[35] and the generation of secondary GWs[36] are presently being examined.

---

[34] G. A. Palma, S. Sypsas, C. Zenteno, Phys. Rev. Lett. **125**, 121301, (2020);
J. Fumagalli, S. Renaux-Petel, J. W. Ronayne, L. T. Witkowski, arXiv:2004.08369 [hep-th].

[35] See, for example, M. Taoso and A. Urbano, JCAP **08**, 016 (2021).

[36] P. Adshead, K. D. Lozanov and Z. J. Weiner, JCAP **10**, 080 (2021);
H. V. Ragavendra, Phys. Rev. D **105**, 063533 (2022).

Thank you for your attention